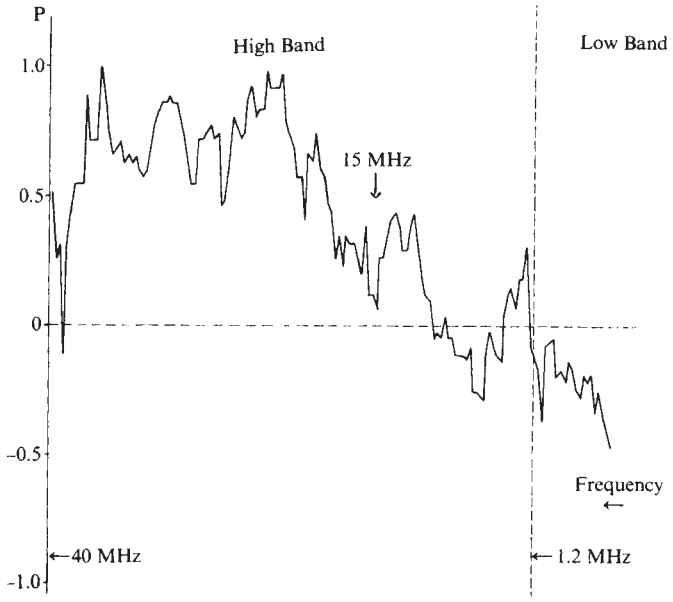

Fig. 5 Polarization as a function of frequency for post-encounter episode. Frequency runs between 40 MHz at left to ~800 kHz at right. A three-point running mean has been used to smooth the curve. Very few points were available at the top of the high band, but at other frequencies above about 15 MHz (marked with arrow) most bursts are clearly left-circularly polarized. Below 15 MHz there is little evidence for any systematic sense of polarization.

which does not appear to be present after the encounter. There is some evidence that this could be due to a smaller source of SED revolving about the planet with a longer period (~10 h 30 min). Pre-encounter, the two sources are just resolved. During the period displayed in Fig. 2 the faster source catches up with, and may overtake, the slower source, and so for the strongest episodes (numbers 3–9), the two are unresolved. In support of this, the early episodes seem to have a slightly greater angular width than the later ones. Support for a two-source model comes from an investigation of the intensity characteristics of the bursts detected in the high rate mode, which exhibit results typical of the superposition of two or more populations (Fig. 3). This hypothesis cannot be rigorously checked until the Voyager 2 encounter.

In the normal mode, the PRA receiver is sensitive to circular polarization. The sense of polarization sampled alternates from channel to channel as a 6-s scan progresses. (Alternating 6-s scans start with alternating polarization sampling of the first channel.) Consequently, should a given SED event show circular polarization, it would appear as a streak of alternating light and dark squares on a dynamic spectrum plot. A search for this phenomenon yielded many examples, such as shown in Fig. 4. We defined an index of polarization for the ith channel, $P(i)$, by

$$P(i) = (L(i) - R(i))/(R(i) + L(i))$$

where $R(i)$, $L(i)$ are the number of 30 ms samples of right-hand and left-hand polarization of the ith channel in which an SED signal was detected. An examination of the SED on the basis of polarization showed that episodes 1–5 contained very few clearly polarized events out of many thousands. Post-encounter episodes, however, were generally strongly left-hand circularly polarized. Polarization/frequency plots were produced for each episode. Figure 5 shows the results for the first post-encounter episode. The SED are clearly strongly left-circularly polarized above ~15 MHz. Below this frequency, the degree of circular polarization is much less, and the sense is frequency-dependent.

We have previously citeh nn on polarization as being evidence of a discharge[2]. Despite the present finding, we still believe that we are observing electrostatic discharges, which are polarized by virtue of either magnetic or curved electric fields, and consequently we have retained the term 'SED'.

In conclusion, some eight characteristics have now been fairly well defined by the Voyager 1 encounter:

(1) a very flat, broadband frequency spectrum;
(2) a period of ~10 h 10 min;
(3) a change in the envelope shape of episodes between pre- and post-encounter;
(4) an intensity population structure typical of plural populations;
(5) episodic structure of width ~180°;
(6) post-encounter episodes continue for about three times as long as pre-encounter ones;
(7) post-encounter bursts are left-circularly polarized at high frequencies;
(8) at least one episode shows the onset of high frequency events some time before that of lower frequency ones.

Any theory for the generation of SED should account for all these characteristics.

We thank other members of the PRA team for helpful suggestions and criticisms of this work. It was supported by NASA-Jet Propulsion Laboratory.

Received 13 May; accepted 15 July 1981.

1. Kaiser, M. L., Desch, M. D. & Lecacheux, A. *Nature* **292**, 731–733 (1981).
2. Warwick, J. W. *et al. Science* **212**, 239–243 (1981).
3. Lang, G. J. & Peltzer, R. G. *IEEE Trans.* **AES-13**, 466–471 (1977).

X-ray and energetic neutral particle emission from Saturn's magnetosphere

E. Kirsch*, S. M. Krimigis†, W. H. Ip* & G. Gloeckler‡

*Max-Planck Institute for Aeronomy, D-3411 Katlenburg-Lindau 3, FRG
† Applied Physics Laboratory, The Johns Hopkins University, Laurel, Maryland 20707, USA
‡ Department of Physics and Astronomy, University of Maryland, College Park, Maryland 20742, USA

Although Voyager 1 was not equipped for the detection of X-rays and neutral particles, its low energy charged particle detector (LECP) records suggest a significant flux of these radiations. X-rays could be due to substantial precipitating electron fluxes in the auroral region or the rings whereas energetic neutrals could be due to charge-exchange between trapped ions and Saturn's neutral hydrogen disk.

THE production of auroral X rays and energetic neutral particles is well known in the Earth's magnetosphere (X rays[1]; charge exchange energetic neutral particles[2–5]) and can be expected at Jupiter and Saturn. In the case of the outer planets, besides charge exchange with the planetary exospheric neutrals, the magnetospheric particles are also subject to similar loss processes due to interaction with the neutral clouds emitted from satellites[6].

0028–0836/81/340718—04$01.00

We present here observations of the Voyager 1 spacecraft obtained a few days before encounter of the Saturn magnetosphere in November 1980. As Voyager 1 has no special experiment onboard for X-ray and neutral particle detection, we use the sensitivity and directional measurements of the LECP (low energy charged particle) analyser to identify the neutral radiation above the charged particle background.

Method of detection

The method has been outlined earlier[7] and will be summarized only briefly here. The LECP telescope[8] uses a silicon detector of 96.5 μm thickness and 0.08 cm^2 area to accumulate counts in eight separate sectors near the ecliptic plane. Electrons $\lesssim$400 keV are magnetically deflected and cannot reach the detector. A stepwise integration of the X-ray sensitivity of the silicon detector for channel PL01 which has an electronic threshold of 26–31 keV, yields an average sensitivity $\bar{\varepsilon}_1 \approx$ 2.38%/keV, and for channel PL02 $\bar{\varepsilon}_2 \approx 0.8\%$/keV ($E = 31$–60 keV). The detection process for energetic neutral particles is the same as for charged particles: the neutrals become ionized when they hit the detector surface and deposit their energy through ionization energy loss in the detector.

The energy thresholds for neutral or charged particles are:

PL01: 40–53 keV ($\varepsilon \approx 0.4$)

PL02: 53–85 keV ($\varepsilon \approx 1$)

PL03: 85–139 keV ($\varepsilon \approx 1$)

Figure 1 shows the trajectory of Voyager 1 for days 307–330, 1980 and the viewing directions of the eight sectors of the instrument. It can be seen that X rays and energetic neutrals escaping from the magnetosphere should appear in sector 5. Encounter of the bowshock[9] occurred at ~23:26 UT on day 316 (11 November 1980), thus the days before 316 can be used for our study. Criteria for the identification of neutral radiation during the pre-encounter phase (Fig. 1 and Kirsch *et al.* unpublished data) can be summarized as follows:

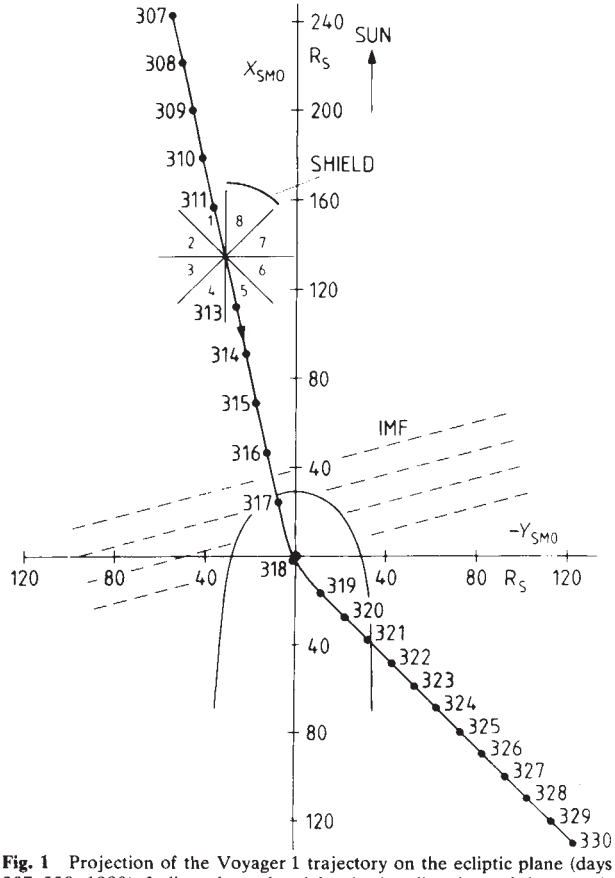

Fig. 1 Projection of the Voyager 1 trajectory on the ecliptic plane (days 307–330, 1980). Indicated are the eight viewing directions of the experiment. Sector 8 is permanently blocked by an aluminum shield.

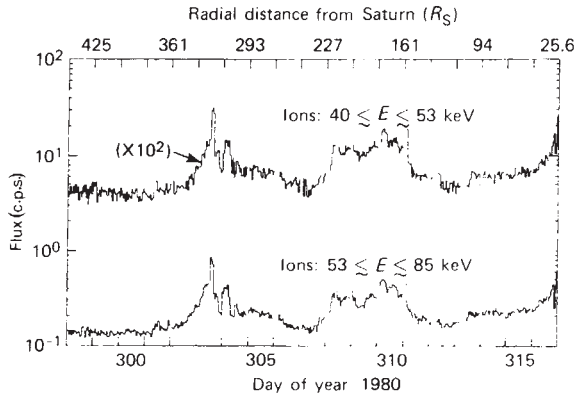

Fig. 2 Scan-averaged measurements of the ion channels PL01 and PL02 for days 298–316, 1980. Interplanetary particle acceleration by Corotating Interaction Regions (CIR) are evident beginning on days 302 and 308.

(1) The interplanetary magnetic field must be nearly perpendicular to the Saturn–Sun line (in the nominal direction) to exclude charged particles escaping from the planet.
(2) The pre-encounter measurements must not be disturbed by solar particles or particles accelerated in corotating structures (CIR) in the interplanetary medium.
(3) Statistically significant enhancements above normal background must appear in the sector which is pointing towards the planet.
(4) The energy spectrum measured within the sector pointing towards the planet should exhibit differences from spectra measured in the other sectors.
(5) The additional flux (after subtracting background) must show a $1/R^2$ dependence (R distance from the planet).

The magnetometer data (ref. 10 and N. F. Ness, personal communication) show the interplanetary magnetic field direction to be almost perpendicular to the Saturn–Sun line, which satisfies criterion (1). To investigate the remaining criteria we show in Fig. 2 the scan-averaged particle measurements for days 298–314. Days 298–300 show the lowest count rates, which are probably due to penetrating galactic cosmic rays. Days 301–305 and 308–311 must be excluded due to the presence of ions associated with typical CIRs (see criterion (2)). On days 313–314 a slight increase was observed which is probably due to solar particles. Thus, we shall examine days 298–300, 306–307, 312–316 (~07:00 UT) in the context of criteria (3)–(5) for the presence of neutral radiation.

Observations

Figure 3*a* shows the sector count rates of channels PL01, 2, 3 for the selected days and the net flux (ΔP) for these channels after the galactic cosmic-ray background was subtracted. Figure 3*b* shows the count rate ratios before, and Fig. 3*c* after, subtraction of the galactic background flux (average of days 298, 299 and 300 has been used as galactic background). From day 312 onward sector 5 shows an increase in comparison with the neighbouring sectors which is ~4 times the statistical error. However, similar peaks exist in sector 1 throughout this period, and in sector 7 from day 313 onwards. Because both of these sectors are generally viewing the solar direction (Fig. 1), we attribute their response to low level fluxes of energetic solar–interplanetary particles. The solar background complicates our detection method. As pointed out in Fig. 1, sector 8 is an experiment calibration sector and cannot be used for further diagnostics of the solar particle contribution. Enhanced fluxes in sector 1 for channels PL02, 3 are most likely produced by the $\vec{E} \times \vec{B}$ drift. The enhanced rate in PL01, sector 1, is due to residual sensitivity to solar X rays, as the Sun was viewed by this sector at this time.

A clue to the identity of the observed fluxes can be obtained by examining the directional energy spectra through the channel ratios. It is evident from the channel ratios presented in Fig. 3*b* (background included) and especially Fig. 3*c* (background subtracted) that the additional flux counted in sector 5 has a

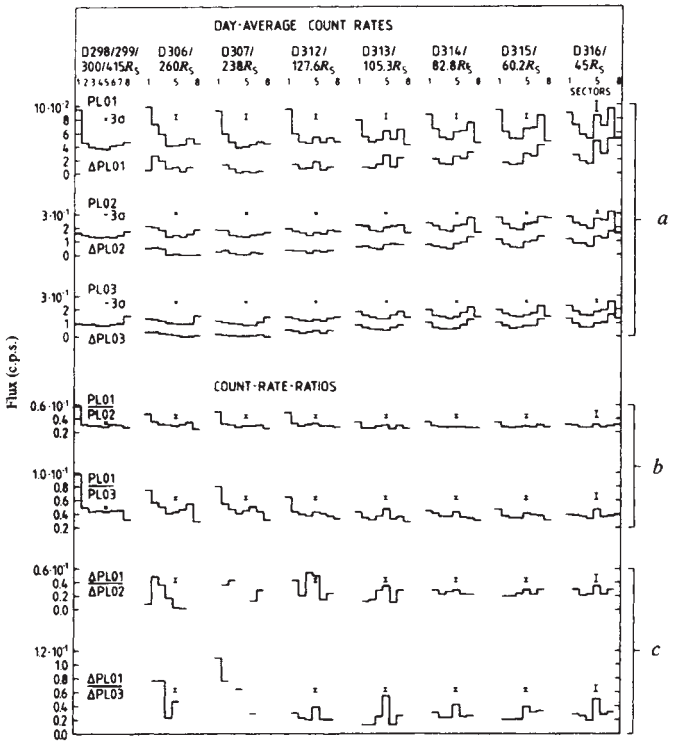

Fig. 3 *a*, Sector-averaged measurements for the days indicated for channels $PL0_{1,2,3}$. $\Delta PL0_{1,2,3}$ indicates that the galactic background is subtracted. The bars on sector 5 represent 3 times the statistical error. *b*, The count rate ratios PL01/PL02, PL01/PL03. *c*, ΔPL01/ΔPL02, ΔPL01/ΔPL03 (after background subtraction) show that sector 5 measured an additional flux which has a softer spectrum than the flux in neighbouring sectors.

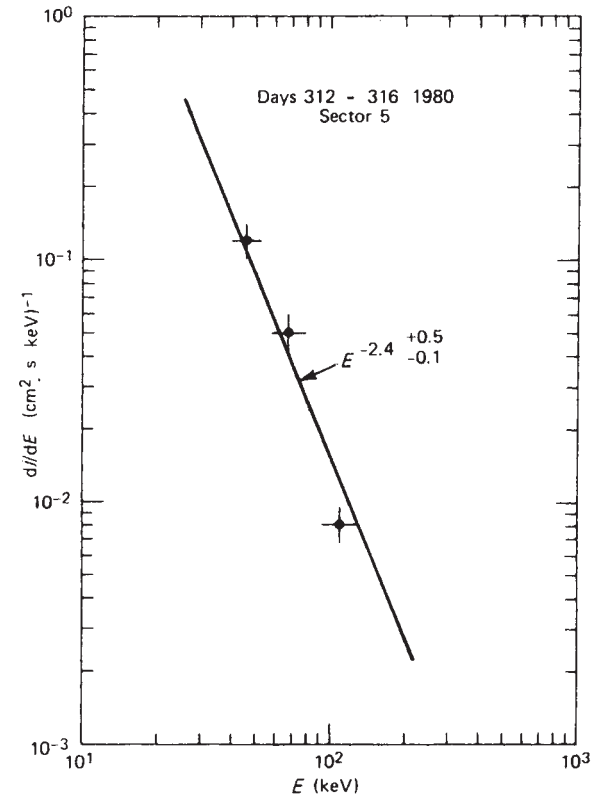

Fig. 4 Differential energy spectrum of the excess radiation, on the assumption that the detector response is due to energetic neutral hydrogen (Table 1).

softer spectrum than the flux of the neighboring sectors. As sectors 6, 7, 1, 2 and probably 3 are most likely to contain interplanetary particles, we compare sector 5 to only sector 4, in an attempt to estimate the additional flux in 5, as follows:

$$\Delta P_{1,2,3} = [(S_5 - S_4) - (Sq_5 - Sq_4)]_{1,2,3} \quad (1)$$

where $S_{5,4}$ are sector count rates and Sq_5, Sq_4 the quiet time sector rates averaged over days 298, 299 and 300. The excess count rates obtained by use of equation (1) are then normalized by multiplication with $(R/45\ R_S)^2$ and listed in Table 1. The statistical errors have been calculated as

$$(\bar{\sigma}_{1,2,3})^2 = \{(\overline{\delta S_4})^2 + (\overline{\delta S_5})^2 + (\overline{\delta Sq_4})^2 + (\overline{\delta Sq_5})^2\}^{1/2} \quad (2)$$

where

$$(\overline{\delta S_{4,5}})^2 = \frac{1}{5}\sum_{n=1}^{5} (\delta S_{4,5})_n^2 \left(\frac{R}{45R_S}\right)_n^2 \quad (3)$$

with $n = 1$ to 5 representing days 312 to 316, 1980, and δSq_4, δSq_5 are the statistical errors of the quiet days average 298, 299 and 300. The errors in the count rate ratios in Fig. 3*b*,*c* shown for each day were calculated using an equation similar to equation (2). Table 1 contains the normalized count rates $\Delta P_{1,2,3}$, the corresponding fluxes and the statistical errors calculated with equation (2). Note that the r.m.s. scatter in the rates for ΔP_1 is larger than the statistical error, and is likely to be due to time variations in this softest part of the spectrum.

The averaged excess count rates in sector 5 shown in Table 1 are statistically significant. The additional counts could be due to planetary or ring X rays, energetic neutrals and/or interplanetary charged particles reflected off the bow shock, so that only upper limits for the neutral radiation can be derived. The averaged X-ray flux j_X can be calculated from the count rate by

$$j_X = \frac{\Delta P_{1,2,3}}{A\varepsilon_X \Delta E_X} \quad (4)$$

where A is detector area, ε_X is X-ray efficiency and ΔE_X is the electronic channel width. Similarly, the neutral particle flux j_n can be calculated from equation (4), but using the appropriate values for ε and ΔE. The results, normalized to a distance of 45 R_S from the planet, are included in Table 1.

Discussion

The significance of the fluxes listed in Table 1 must be examined in the context of processes known or expected to take place in the vicinity of Saturn. Production of X rays can occur in auroral processes recently observed to take place at Saturn[11] over a relatively narrow range in latitude, 78°–81.5°. If the electron precipitation takes place over the area of the observed UV signature ($A \sim 10^{19}$ cm^2, that is, 2% of the surface), then the emitted photon flux at the source is given by

$$j_X < \frac{j_X 4\pi R^2\, \Delta E}{A} = 3.4 \times 10^6 \text{ photons cm}^{-2}\text{ s}^{-1} \quad (5)$$

with $\Delta E \sim 7$ keV, $R = 45\ R_S$. The corresponding electron flux

Table 1 Excess rates, fluxes in sector 5 (normalized to 45 R_S)

Day (normalization)*	ΔP_1(c.p.s.)	ΔP_2(c.p.s.)	ΔP_3(c.p.s.)
312 (8.1)	7.89×10^{-2}	1.66×10^{-1}	7.5×10^{-2}
313 (5.44)	7.38×10^{-2}	1.69×10^{-1}	
314 (3.4)	4.16×10^{-2}	1.38×10^{-1}	2.4×10^{-2}
315 (1.78)	2.80×10^{-2}	0.79×10^{-1}	2.1×10^{-2}
316 (1.0)	3.43×10^{-2}	0.76×10^{-1}	2.5×10^{-2}
Ave† (c.p.s.) $\pm 1\sigma$	0.051 ± 0.008	0.126 ± 0.014	0.36 ± 0.012
Flux (counts cm^{-2} s^{-1})	0.64 ± 0.1	1.57 ± 0.18	0.46 ± 0.15
j_X(photons cm^{-2} s^{-1} keV^{-1})	5.4 ± 0.9	6.1 ± 0.7	
j_n(cm^2 s keV)$^{-1}$	0.12 ± 0.02	0.05 ± 0.01	0.008 ± 0.003
Energy range (keV)			
X rays	26–31	31–63	63–121
Neutrals/charged	40–53	53–85	85–139

* Factors in parentheses are obtained from $(R/45\ R_S)^2$ and are used to normalize the excess rate to 45 R_S.
† Averages normalized to 45 R_S.

precipitating into the atmosphere can be estimated by using a conversion efficiency of $\sim 2\times10^{-5}$ photons per electron[12]; we find $J\sim 1.7\times10^{11}$ electrons cm^{-2} s^{-1} which is some 10^3 larger than the maximum fluxes measured by the LECP experiment within the magnetosphere of the planet[13]. Hence, we conclude that the observed upper limit, if interpreted in terms of X rays, cannot be reasonably related to precipitating magnetospheric electrons. The same conclusion is reached even if precipitation is assumed to occur over the entire visible hemisphere.

Another possible X-ray source is the interaction of radiation belt electrons with the rings of Saturn, which extend out to $\sim 2.5\ R_S$. The surface area of the rings on the sunlit side is

$$S=(2.5\ R_S)^2\pi-(1\ R_S)^2\ \pi\simeq 6\times10^{20}\ \text{cm}^2 \qquad (6)$$

If we assume ~1% of the area to be filled with matter, the estimated X-ray production in the rings in the energy range 31–63 keV (PL02), is

$$J_X=\frac{6.1\times4\pi(43\ R_S)^2\times32}{6\times10^{18}}=2.7\times10^7\ \text{photons cm}^{-2}\ \text{s}^{-1} \qquad (7)$$

The corresponding electron precipitation is $\sim 1.4\times10^{12}$ cm^{-2} s^{-1}, again $\sim 10^4$ larger than the maximum flux measured by the same instrument in the magnetosphere with this channel[13]. Note that there is a sharp cutoff in particle fluxes at the edge of ring A, as shown by Pioneer 11[14].

The Voyager 1 UV experiment[11] found that Saturn is surrounded by a torus of neutral hydrogen with a concentration $n_H\approx 10$ cm^{-3}. The torus extends from $\sim 25\ R_S$ to $\sim 8\ R_S$ and its thickness could be $\sim 6\ R_S$. Thus charge exchange processes between radiation belt protons and the neutral hydrogen concentration can be expected. For a flux estimation we use the cross-sections given by Tinsley[5]. The product σv (cross-section × velocity of the particles) is as follows for the lowest three channels

PL01: (40–53 keV): $\sigma v_H^+\approx 3\times10^{-8}$ cm^3 s^{-1}

PL02: (53–85 keV): $\sigma v_H^+\approx 1.4\times10^{-8}$ cm^3 s^{-1}

PL03: (85–139 keV): $\sigma v_H^+\approx 3\times10^{-9}$ cm^3 s^{-1}

The lifetime against charge exchange is then

PL01: $\tau_1=(n_H\sigma v)^{-1}=(10\times3\times10^{-8})^{-1}=3.33\times10^6$ s

PL02: $\tau_2=(n_H\sigma v)^{-1}=(10\times1.4\times10^{-8})^{-1}=7.14\times10^6$ s

PL03: $\tau_3=(n_H\sigma v)^{-1}=(10\times3\times10^{-9})^{-1}=3.33\times10^7$ s

The LECP instrument measured an average density outside the orbit of Rhea at $E\gtrsim 40$ keV of $\sim 5\times10^{-3}$ cm^{-3} (ref. 13). Taking the neutral hydrogen cloud volume of $\sim 2\times10^{33}$ cm^3 (ref. 11) we can estimate the total energetic ion content as

$$N=nV=5\times10^{-3}\ \text{cm}^{-3}\times2\times10^{33}\ \text{cm}^3=10^{31}$$

The total energetic neutral particle production is given by

$$\dot N=\frac{nV}{\tau}=\frac{10^{31}}{10^7}=10^{24}\ \text{neutrals s}^{-1}$$

The loss rate may be obtained by estimating the total surface area of the neutral hydrogen disk,

$$A\simeq 2\pi[(25\ R_S)^2-(8\ R_S)^2]\simeq 1.3\times10^{23}\ \text{cm}^2$$

Thus energetic ($E\gtrsim 40$ keV) neutrals are lost at a rate

$$\frac{\dot N}{A}=\frac{10^{24}}{1.3\times10^{23}}\sim 8\ \text{cm}^{-2}\ \text{s}^{-1}$$

The flux at 45 R_S would be decreased by a factor $\sim(20/45)^2=0.2$, that is, $\dot N/A$ would be ~ 1.6 cm^{-2} s^{-1}.

We now need to compare the expected flux at 45 R_S with the observations as summarized in Table 1. The differential flux from Table 1 has been plotted in Fig. 4; the form of the spectrum can be described by a power law of the form $E^{-\gamma}$ with $\gamma\sim 2.4$. To obtain the total flux we evaluate the integral

$$J=\int_{40\ \text{keV}}^{\infty}KE^{-2.4}\,dE$$

and find $J\sim 4.3$ cm^{-2} s^{-1}. This value compares well with the expected value of ~ 1.6 cm^{-2} s^{-1} derived above.

We have demonstrated the existence of radiation above the detector background emanating from the vicinity of Saturn, upstream from the bow shock. The excess counts are most plausibly attributed to neutral radiation, that is, X rays and/or neutral energetic particles. Estimates of the number of energetic electrons necessary to produce the observed counts by precipitation in either the saturnian auroral regions or the rings are too high by factors $\sim 10^3$–10^4 over electron intensities observed within the magnetosphere of Saturn. Thus the observed excess counts are probably not due to X rays even if satellite surfaces are considered as possible X ray sources. We conclude that charge exchange of energetic ions with satellite tori is an important loss mechanism at Saturn as well as at Jupiter[15].

The efforts of many at APL/JHU, the Universities of Maryland and Kansas and Bell Laboratories contributed to this investigation. We thank our colleagues on the LECP team: T. P. Armstrong, W. I. Axford, C. O. Bostrom, E. P. Keath and L. J. Lanzerotti for various contributions, J. F. Carbary for assistance with graphics, and especially L. J. Lanzerotti for useful comments. This research was supported in part by NASA under Contract N00024-78-C-5384 between The Johns Hopkins University and the Department of the Navy, and under subcontract to the University of Maryland.

Received 13 May; accepted 7 July 1981.

1. Kremser, G. *Scientific Ballooning* (ed. Riedler, W.) 161 (Pergamon, Oxford, 1979).
2. Moritz, J., *J. geophys. Res.* **38,** 701 (1972).
3. Hovestadt, D., Haeusler, B. & Scholer, M. *Phys. Rev. Lett.* **28,** 1340 (1972).
4. Blake, J. B. *J. geophys. Res.* **81,** 6189 (1976).
5. Tinsley, B. A. *J. geophys. Res.* **81,** 6193 (1976).
6. Cheng, A. F. *Astrophys. J.* **242,** 812 (1980).
7. Kirsch, E., Krimigis, S. M., Kohl, J. W. & Keath, E. P. *Geophys. Res. Lett.* **8,** 169 (1981).
8. Krimigis, S. M. *et al. Space Sci. Rev.* **21,** 329 (1977).
9. Bridge, H. S. *et al. Science* **212,** 217 (1981).
10. Ness, N. F. *et al. Science* **212,** 211 (1981).
11. Broadfoot, A. L. *et al. Science* **212,** 206 (1981).
12. Evans, R. D. *The Atomic Nucleus* 619 (McGraw-Hill, New York, 1955).
13. Krimigis, S. M. *et al. Science* **212,** 225 (1981).
14. Van Allen, J. A., Thomsen, M. F., Randall, B. A., Rairden, R. L. & Grosskreutz, C. L. *Science* **207,** 415 (1980).
15. Cornwall, J. M. *J. geophys. Res.* **77,** 1756 (1972).

Topology of Saturn's main magnetic field

M. H. Acuña, J. E. P. Connerney & N. F. Ness

NASA/Goddard Space Flight Center, Laboratory for Extraterrestrial Physics, Greenbelt, Maryland 20771, USA

The Voyager 1 magnetic field observations at Saturn confirm the principally dipolar topology of the planetary magnetic field and suggest the need for more general models which incorporate non-potential field sources external to the planet and within the planetary magnetosphere.

THE close flyby of Saturn at 3.07 R_S (1 R_S = 60,330 km) by Voyager 1 in November 1980 provided a second opportunity to study *in situ* the intrinsic planetary magnetic field. The first detection of the Saturnian field was accomplished by experiments aboard Pioneer 11 during its close flyby of Saturn at 1.35 R_S in September 1979[1–4]. The most surprising

0028-0836/81/340721—04$01.00